Journal of the Serbian Chemical Society
JSCS-info@shd.org.rs • www.shd.org.rs/JSCS
J. Serb. Chem. Soc. *90* (9) 1027–1040 (2025)
JSCS–5437
Original scientific paper
Published 30 September, 2025

Binding elucidation of azo dye with DNA *via* spectroscopic approaches and molecular docking techniques

SHABNAM JAMPOUR-KOLOUR and HAMID DEZHAMPANAH*

Department of Applied Chemistry, Faculty of Chemistry, University of Guilan, P.O.B. 1914, Rasht 0098, Iran

(Received 23 March; revised 10 April; accepted 16 July 2025)

Abstract: In this study, the interaction between a synthesized monoazo disperse dye and calf thymus DNA (Ct-DNA) was investigated *via* UV–Vis spectroscopy, fluorescence and FT-IR spectroscopy and molecular docking calculations. Hypochromic effects on the absorbance and quenching of fluorescence were observed, revealing the binding of azo dye to Ct-DNA. Upon the addition of Ct-DNA, the azo dye showed a hypochromic effect and a small redshift in the wavelength of the absorption spectra, suggesting a groove binding mode of interaction of this probe with Ct-DNA, which was confirmed by the molecular docking results. The values of the binding constant were calculated from the maximum absorption spectra of the azo dye at various Ct-DNA concentrations at several temperatures and the corresponding thermodynamic parameters $\Delta G°$, $\Delta H°$ and $\Delta S°$ were obtained. In addition, fluorescence resonance energy transfer showed that the distance between the donor (EB–Ct-DNA) and acceptor (azo dye) is suitable for energy transfer. Molecular docking analysis revealed that hydrogen bonds and π-electrons on the benzene ring of the azo dye are crucial for binding the azo dye to Ct-DNA. The results of the molecular docking investigations corroborate well with those of the spectral studies and these probes bind to the minor groove of Ct-DNA.

Keywords: calf thymus DNA; fluorescence spectroscopy; molecular modeling; UV–Vis spectroscopy; synthesized azo dyes.

INTRODUCTION

Deoxyribonucleic acid (DNA) and ribonucleic acid (RNA) are the two main forms of nucleic acid. All living organisms, including multicellular mammals and single-celled bacteria, have DNA as their genetic material.[1] DNA is a medium for storing information. For DNA to serve this purpose and maintain information

* Corresponding author. E-mail: h.dpanah@guilan.ac.ir
https://doi.org/10.2298/JSC250328047J

for an organism's lifetime, which for certain trees may span many millennia, it must be incredibly stable. DNA is found in the nucleus of eukaryotic cells, as well as in organelles such as mitochondria and chloroplasts. Like most biological molecules, the structure of DNA is closely related to its function, which involves storing genetic information.

A single strand can always be converted into a complimentary strand owing to the particular hydrogen bond pairing between the GC and AT bases. While these hydrogen bonds help stabilize the double helix structure, they can be disrupted when the DNA needs to be accessed.[2]

When proteins are translated, the information needed to code for amino acids is contained in the base sequence. Through interactions with proteins involved in DNA packaging and regulation, DNA sequences that do not directly encode amino acids can transmit crucial information. The sequences that are accessible to DNA-interacting proteins can vary according to the major and minor grooves of DNA.[3]

DNA serves as a crucial intracellular target, making the design and synthesis of DNA-binding ligands an important area of focus in cancer therapy. The binding of these ligands can cause significant changes in the locations and affinities of DNA binding modes. This offers critical information for creating DNA probes specific to certain sites and possible chemotherapeutic drugs.[4] In recent years, extensive research has been conducted on the interactions between bioactive molecules and DNA, as these studies offer insights into the origins of diseases and the structural properties of DNA and contribute to the design of new chemotherapeutic agents.[5]

Azo dyes are the oldest and most widely used class of industrially manufactured organic dyes because of their many uses in biological research and applications and in the coloring of textiles, leather, paper, food and cosmetic items. Additionally, they are employed in high-tech fields such as dye-sensitized solar cells, lasers and photodynamic treatment.[6] Azo dyes, particularly azo dispersion dyes, contain hydrogen atoms in their molecules; they are traditionally utilized primarily for their classical application in dyeing fibers, for example. In the research of solvent and substituent effects on the λ_{max} values of produced dyes, azobenzene dyes with donor and acceptor terminal groups in conjugated systems of dyes have been used and applied in recent years.[7] These dyes demonstrate notable biological properties and their antibiotic, antifungal and anti-HIV effects render them highly valuable in medicinal chemistry. However, despite their broad applications, azo dyes are known to be carcinogenic when they interact with DNA, leading to mutations.[8–10]

Many studies conducted recently have concentrated on the synthesis and structural characteristics of azo dyes. These advancements have inspired inorg-

anic chemists to explore new techniques for developing more effective and targeted drugs involving azo dyes.[11–13]

The intriguing physicochemical properties of azo compounds have made them compelling subjects of study in physical biochemistry. Their potential to interact with biomolecules such as DNA through intercalation or groove binding offers a unique platform for exploring fundamental molecular interactions. Investigating these interactions not only enhances our understanding of DNA–drug binding mechanisms but also contributes to the rational design of bioactive compounds with diagnostic or therapeutic applications.[14] Therefore, this study aims to bridge the gap between synthetic azo chemistry and the biophysical exploration of Ct-DNA interactions.

In the present research, the molecular details of the interaction between the synthetic azo dye (Scheme 1) and calf thymus DNA (Ct-DNA) were investigated systematically via various spectral techniques, such as synchronous fluorescence, Fourier transform infrared (FT-IR) spectroscopy, ultraviolet–visible spectroscopy and molecular docking studies. The main objectives, therefore, of the present study are to determine the binding constant, binding mode, Stern–Volmer constant (K_{SV}) and rate constant for quenching (k_q), which can be determined by optical absorption, fluorescence spectroscopy and molecular docking. A complete understanding of the BAE–Ct-DNA binding mechanism and the factors that influence it would contribute to the design of new anticancer, antiviral and antibacterial drugs. The chemical structure and IUPAC name of this mono-azo disperse dye derivative are given in Scheme 1, and the abbreviation BAE is used in this document.

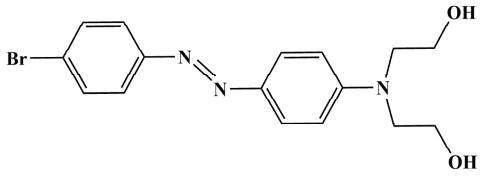

Scheme 1. Molecular structure of (*E*)-2,2'-((4-((4-bromophenyl)diazenyl)phenyl)azanediyl)-bis(ethan-1-ol) (BAE).

EXPERIMENTAL

Materials

Calf thymus DNA from Sigma–Aldrich was dissolved in double-distilled water and stored in the dark at 4 °C. The Ct-DNA solution concentration (3.44×10^{-3} M) was determined *via* an extinction coefficient of 13200 M^{-1} cm^{-1} at 260 nm.[15]

The azo dye BAE was synthesized based on established literature.[16] A stock solution of the azo dye (2×10^{-3} M) was prepared in ethanol and then diluted with 5 mM phosphate buffer to the final concentration. The dye solution was stored in the dark at 4 °C and used fresh after preparation. All the analyses were conducted with 5 mM phosphate buffer at pH 7.20.[17]

UV–Vis absorption spectroscopy

A UV–Vis spectrometer was used to record absorption spectra under simulated physiological conditions (pH 7.2) *via* an Agilent Technologies UV-1601 spectrophotometer. The absorption measurements were taken at a constant concentration of azo dye (67.63 μM) and various concentrations of Ct-DNA (0–31 μM) across temperatures ranging from 298.2 to 313.2 K. A 10 mm quartz cell was employed for measurements in the wavelength range of 300–550 nm. The UV–Vis titration experiments were conducted by adding the Ct-DNA stock solution to a 1 ml cuvette containing the azo dye solution at the appropriate concentration.

Fluorescence spectroscopy study

Similar to the absorption spectra titration experiments, the emission spectra of ethidium bromide (EB) bound to Ct-DNA in the absence and presence of BAE were recorded using a Varian Cary Eclipse spectrofluorometer. A 1.5 ml sample of an EB solution with a fixed concentration (70 μM) was mixed with 330 ml of Ct-DNA solution (209 μM) in a 10 mm quartz cuvette at 25 °C. The mixture of EB–Ct-DNA was titrated with 5 to 463 μl of BAE solution in phosphate buffer. The solutions were excited at 450 nm, and the emitted light intensity was measured at 550–700 nm. The temperature was held constant at ±1 °C during the titration experiments.

The fluorescence intensity of EB–Ct-DNA complex was corrected for the inner filter effect using the following equation:[18]

$$F_{cor} = 10^{(A_1+A_2)/2} F_{obs} \quad (1)w$$

where F_{cor} is the corrected fluorescence intensity, F_{obs} is the observed fluorescence intensity in the experiment, and A_1 and A_2 are the total absorbances of all the components at the excitation wavelength (λ_1) and the emission wavelength (λ_2), respectively.

FT-IR spectroscopic measurements

FT-IR measurements were conducted at room temperature using an Alpha FT-IR spectrometer (Bruker). The Ct-DNA concentration was constant at 500 μM, while the dye concentration was 40 μM. The pellets were prepared by mixing the freeze-dried samples with KBr and compressing them under vacuum for 3 min.[19]

Energy transfer measurements

FRET is broadly used to assign proximities, distances, orientations and dynamic properties of biomolecular structures. The absorption spectrum of BAE and the fluorescence spectrum of DNA–BAE were recorded, covering a wavelength range of 530–700 nm with 12.10 μM of BAE and DNA at 298.2 K.

Molecular docking

Molecular docking is an effective technique for understanding the interaction between ligands and biological targets and is crucial for clinical treatment and the recognition of nucleic acid molecules.[20] In this case, AutoDock 4.2 software was used to study molecular docking.[21] The 3D structure of BAE was determined via Gauss View 5.0. The geometry of the BAE ligand was optimized *via* density functional theory (DFT) (B3LYP/6-31G*(d,p)) *via* Gaussian 03. Additionally, the Ct-DNA structure was taken from the protein data bank (http://rcsb.org, PDB ID: 1bna); then, all the ligands and water molecules were removed and hydrogen atoms were added. Here, AutoDock tools software was used to convert DNA and ligands to pdbqt format, and the connection between the two was performed *via* AutoDock Vina software. The grid box used in this study was defined with dimensions of 30 Å×30 Å×50

Å and a grid spacing of 1 Å, centered at coordinates (15.422, 21.448, 8.999). Finally, the model and binding sites were evaluated *via* Discovery Studio, and the atoms in the hydrogen bonds and hydrophobic residues in the complex were evaluated *via* Ligaplot.

RESULTS AND DISCUSSION

UV–Vis study of the BAE interaction with Ct-DNA

UV–Vis spectroscopy is an easily available technique for investigating ligand-binding reactions, enzyme catalysis and conformational change transitions in proteins and nucleic acids.

The changes in the absorption spectra of dye (ligand) in terms of wavelength changes, hyperchromic/hypochromic effects, and isosbestic points can be used to study the interactions of certain functional groups with $\pi \rightarrow \pi^*$ and $n \rightarrow \pi^*$ transitions with Ct-DNA. These spectrum characteristics result from molecular interactions that are intimately linked to variations in bonding energy levels.[22]

Generally, hyperchromic/hypochromic are the two spectral features, which are closely related to the double helix structure of Ct-DNA.[23] The hyperchromic effect (increase in absorption of the DNA band) and the hypochromic effect (decrease in absorption of the Ct-DNA band) are the spectral changes typical of the interaction of a compound with Ct-DNA helix. Hypochromic effect results from contraction of the Ct-DNA helix as well as changes in its conformation, while hyperchromic effect is due to the damage to the Ct-DNA double helix structure. Moreover, the binding of an intercalative molecule to Ct-DNA is accompanied by hypochromic effect (30 %) and a significant red shift (> 15 nm) is characteristic of strong π–π stacking interaction between the aromatic chromophore of the ligand and Ct-DNA base pairs. On the other hand, groove binding results only in a small shift and moderate hypochromic effect in the absorption spectra.

The characteristic change in the maximum absorption wavelength of BAE (454 nm) during the titration of Ct-DNA is shown in Fig. 1. Upon the addition of varying concentrations of Ct-DNA, the absorption intensity gradually decreases and shifts to longer wavelengths (bathochromic shift) by approximately 3 nm in terms of the absorption maxima, indicating a shift to a more polar environment upon interaction. These remarkable hypochromic effects and small red shift indicate the existence of strong interactions between BAE and Ct-DNA, most likely *via* the groove binding mode. These spectral properties indicate a high affinity of the complex for binding to Ct-DNA.

On the basis of the changes in the absorbance of BAE at 454 nm during titration with Ct-DNA, the intrinsic binding constant (K_b) between BAE and Ct--DNA was calculated *via* following equation:

$$\frac{A_0}{A - A_0} = \frac{\varepsilon_d}{\varepsilon_{H\text{-}d} - \varepsilon_d} + \frac{\varepsilon_d}{\varepsilon_{H\text{-}d} - \varepsilon_d} \frac{1}{K_b[DNA]} \quad (2)$$

Here, A_0 and A represent the absorbances of the BAE in the absence and presence of Ct-DNA, respectively. ε_d and $\varepsilon_{H\text{-}d}$ are the corresponding absorption coefficients of free BAE and BAE in the presence of Ct-DNA (fully bound form), respectively. A plot of $A_0/(A–A_0)$ *versus* 1/[DNA] yields a slope of $(\varepsilon_d/(\varepsilon_{H\text{-}d} - \varepsilon_d)(1/K_b)$ and a *Y*-intercept equal to $(\varepsilon_d/(\varepsilon_{H\text{-}d} - \varepsilon_d)$, where K_b is the ratio of the intercept to the slope. The linear plot for the binding of BAE to Ct-DNA is shown in Fig. S-1 of the Supplementary material to this paper, and the intrinsic binding constant, K_b ($(4.91\pm0.04)\times10^6$ L mol^{-1}) at 454 nm was calculated on the basis of the ratio of the intercept to the slope of the corresponding linear equation. The results are shown in Table I at various temperatures ranging from 298.2 to 318.2 K. The observed values of K_b have also revealed that the BAE azo dye binds to Ct-DNA *via* groove mode.[23]

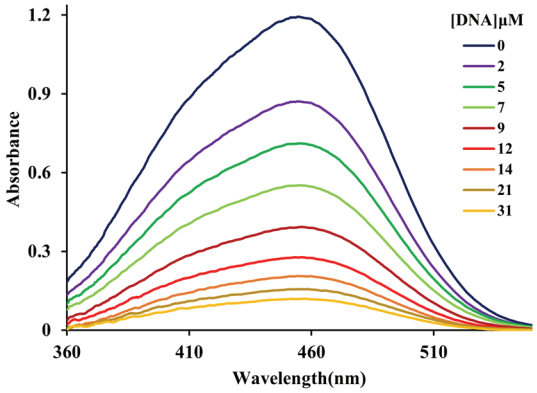

Fig. 1. UV–Vis absorption spectra of Ct-DNA-BAE at 298.2 K in 5 mM phosphate buffer (pH 7.2) with various concentrations of Ct-DNA ranging from 0 to 22.43 μM.

Determination of thermodynamic functions

To facilitate the binding of a small molecule to a biological macromolecule, hydrogen bonding, van der Waals interactions, electrostatic forces and hydrophobic contacts play crucial roles. The primary forces involved in the binding process can be explained by the signs and significance of thermodynamic parameters, such as the entropy change ($\Delta S°$) and enthalpy change ($\Delta H°$). Therefore, the van't Hoff equation was used to evaluate the thermodynamic parameters related to the acquired binding constants:

$$\ln K = -\frac{\Delta H^\circ}{RT} + \frac{\Delta S^\circ}{R} \tag{3}$$

where K is the binding constant at the appropriate temperature, and R and T are the gas constant and absolute temperature, respectively. The effects of temperature variation on the binding constant were investigated at 298.2, 303.2, 313.2

and 318.2 K. The plots of ln *K versus* 1/*T* can be used to determine the values of $\Delta H°$ and $\Delta S°$. The value of $\Delta H°$ can be considered temperature-independent when the temperature varies only slightly. Therefore, Eq. (4) can be used to determine the free energy change ($\Delta G°$):

$$\Delta G^\circ = \Delta H^\circ - T\Delta S^\circ = -RT \ln K \quad (4)$$

Based on the binding constants of BAE to Ct-DNA at various temperatures, the thermodynamic parameters ($\Delta H°$, $\Delta G°$ and $\Delta S°$) were calculated *via* these equations, with the results presented in Fig. S-2 and Table I. The negative values of $\Delta G°$ under all the conditions indicate that the interaction was spontaneous.[24]

TABLE I. Binding constant and thermodynamic parameters for the BAE–Ct-DNA system from UV–Vis data at different temperatures

T / K	$K_b \times 10^{-6}$/ L mol^{-1}	$\Delta H°$ / kJ mol^{-1}	$\Delta S°$ / J mol^{-1} K^{-1}	$\Delta G°$ / kJ mol^{-1}
298.2	4.91±0.04	28.62±0.04	224.10±0.01	–38.17±0.01
303.2	6.07±0.05		224.30±0.02	–39.35±0.01
313.2	8.48±0.06		224.00±0.01	–41.51±0.02
318.2	10.3±0.3		224.20±0.02	–42.69±0.01

The sign and magnitude of the thermodynamic parameters for different types of interactions in protein association processes were described by Ross and Subramanyam.[25] Considering the water structure, a positive value of $\Delta S°$ is commonly considered proof of hydrophobic interactions. The interaction process is spontaneous, as indicated by the negative value of $\Delta G°$. The positive enthalpy and entropy changes of the interaction between BAE and Ct-DNA indicate that the binding is primarily entropy-driven, with enthalpy change being unfavorable for this process. Thus, hydrophobic forces play a major role in the binding BAE to Ct-DNA.[24] Overall, the consistency between the molecular docking results and the thermodynamic data reinforces the reliability of our findings.

Fluorescence studies of Ct-DNA and BAE

Fluorescence quenching measurement is an important method for studying interactions between small molecules and biomolecules. Upon the addition of increasing concentrations of BAE (0–168 μM) to the EB–Ct-DNA system, the fluorescence peak slightly red-shifted at 604 nm, and the intensity of the EB–Ct--DNA system attenuated regularly with increasing concentrations of BAE, which indicated that interactions occurred between BAE and the EB–Ct-DNA system. The results are shown in Fig. S-3 of the Supplementary material. This finding indicated that BAE binding with EB–Ct-DNA formed a new non-fluorescent EB–Ct-DNA–BAE complex, which decreased the fluorescence intensity of EB––Ct-DNA. The results revealed that BAE cannot intercalate into Ct-DNA in the presence of EB. Then, the intensity of the EB–Ct-DNA system fluorescence dec-

reased because BAE bound with EB–Ct-DNA. The fluorescence emission peak slightly red-shifted by 2 nm, but the peak shape did not significantly change, which meant that the microenvironment of the EB had changed and that BAE had reacted with EB–Ct-DNA.[26] To further elucidate the quenching mechanism, fluorescence quenching was examined *via* the Stern–Volmer equation:

$$\frac{F_0}{F} = 1 + K_{SV}[Q] = 1 + k_q \tau_0 [Q] \quad (5)$$

where F_0 and F are the fluorescence intensities of EB–Ct-DNA in the absence and presence of the quencher BAE, respectively; K_{SV} is the Stern–Volmer quenching constant; k_q is the EB–Ct-DNA complex quenching rate constant; τ_0 is the fluorophore's typical lifetime in the absence of BAE (10^{-8} s); and [Q] is the BAE concentration.[27]

Fig. S-4 of the Supplementary material shows the Stern–Volmer plot for the fluorescence quenching of the EB–Ct-DNA complex by BAE, which has good linearity (R^2 = 0.98). The quenching constants K_{SV} and k_q are shown in Table II for BAE, the calculated value of k_q was much greater than the diffusion-controlled quenching rate constant of various quenchers with the biopolymer (2×10^{10} L mol^{-1} s^{-1}) in aqueous medium.[28] Thus, the fluorescence enhancement is not initiated by a dynamic process. It is suggested that a static process involves complex formation in the ground state.[29]

TABLE II. Quenching constants (K_{SV} and k_q) obtained from the fluorescence measurements

Dye	T / K	K_{SV} / L mol^{-1}	k_q / L mol^{-1} s^{-1}	R^2
BAE	298.2	$(1.29\pm0.03)\times10^4$	$(1.29\pm0.03)\times10^{12}$	0.98

Energy transfer between EB–Ct-DNA and BAE

Fluorescence resonance energy transfer (FRET) occurs when the emission spectrum of a fluorophore (donor) overlaps with the absorption spectrum of another molecule (acceptor) and the distance between them is less than 8 nm.[30]

To enhance FRET efficiency, the EB–Ct-DNA complex was used as the energy donor and BAE as the energy acceptor. The distance between the donor and the acceptor can be ascertained *via* FRET measurements. In our experiment, Förster energy transfer was used to determine the binding distance (r) for energy transfer from EB–Ct-DNA and BAE azo dye. The energy transfer parameter can be computed *via* the following equation:[31]

$$E = 1 - \frac{F_0}{F} = \frac{R_0^6}{R_0^6 + r^6} \quad (6)$$

where F_0 and F are the fluorescence intensities of EB–Ct-DNA and BAE–Ct--DNA–EB, respectively. R_0 is the critical distance when 50 % of the excitation energy is shifted to the acceptor. R_0 can be calculated *via* the following equation:[32]

$$R_0^6 = 8.79\times10^{-25} K^2 n^{-4} \phi J \tag{7}$$

This formula includes the dipole's spatial orientation factor (K^2), the medium's refractive index (n), the donor's fluorescence quantum yield (ϕ) and the spectral overlap effect between the donor's emission and acceptor's absorption spectra (J), which is determined *via* the following formula:

$$J = \frac{\int_0^\infty F(\lambda)\varepsilon(\lambda)\lambda^4 \mathrm{d}\lambda}{\int_0^\infty F(\lambda)\mathrm{d}\lambda} \tag{8}$$

In this formula, $F(\lambda)$ is the fluorescence intensity of the donor and $\varepsilon(\lambda)$ represents the molar absorption coefficient of the acceptor at wavelength λ.[33] Fig. S-5a and b of the Supplementary material show the overlap between the absorption spectrum of BAE and the fluorescence emission spectrum of EB–Ct-DNA, which is K^2 = 2/3, n = 1.33 and ϕ = 0.16 for EB–Ct-DNA.[34] According to Eqs. (6)–(8), the parameters J, R_0, E and r were 1.21×10^{13} cm^3 L mol^{-1}, 2.26 nm, 0.10 nm and 2.99 nm, respectively. The value of r is the distance from the BAE to the EB–Ct-DNA, is less than 8 nm and $0.5R_0 < r < 1.5R_0$. This result indicates that the binding obeyed the conditions of Förester's energy transfer theory and energy transfer from EB–Ct-DNA to the BAE has a high probability.[35]

FT-IR studies of Ct-DNA and BAE

To verify the structural changes in Ct-DNA upon the addition of BAE, FT--IR spectroscopy was employed to analyze and examine the secondary structure of both the Ct-DNA and BAE–Ct-DNA complexes. The FT-IR spectra of the BAE–Ct-DNA system at 950–1750 cm^{-1} are presented in Figs. S-6 and S-7 of the Supplementary material. The concentrations of Ct-DNA and BAE were fixed at 500 and 40 μM, respectively. The intensity of the absorption spectra generally significantly increased with the addition of BAE.

The stretching vibrations of C=O and C=N bonds, as well as the bending vibrations of exocyclic –NH_2 groups found in Ct-DNA bases, are the main sources of the first region (approximately 1600–1750 cm^{-1}) of the infrared spectrum of Ct-DNA.[36] Purine and pyrimidine ring vibrations are the main sources of the second region (~1600–1500 cm^{-1}), and the symmetric and asymmetric stretching of PO_2 groups within the phosphodiester-deoxyribose backbone constitutes the third region (~950–1250 cm^{-1}).

Strong bands originating from the carbonyl stretching modes of DNA bases are found in the 1750–1550 cm^{-1} region. These modes are superposed to form the spectrum in this area. Certain bands could have frequencies that are near those of nearby peaks. These summits may be concealed or covert. We used the second derivative approach to perform spectral decomposition for free Ct-DNA and BAE–Ct-DNA, as shown in Figs. S-8 and S-9 of the Supplementary material, to further examine the associated vibrations. Table III summarizes the proposed assignment of the individual vibration bonds of Ct-DNA.

TABLE III. The assignments of individual peaks in the Ct-DNA spectra

Abs.max., cm^{-1}	Band's vibrations of Ct-DNA	Abs.max., cm^{-1}	Band's vibrations of Ct-DNA
1688	C2=O of thymine	1579	C=N(H2) of guanine
1673	C6=O of guanine	1573	C=N7 of guanine
1658	C4=O of thymine	1105	Group PO_2 (symmetrical)
1641	Thymine ring	1058	C–O of deoxyribose
1619	Adenine ring	1028	Deoxyribose ring

The vibrations for the decomposed bands of DNA are C2=O for thymine, C6=O for guanine, C4=O for thymine, the thymine ring, the adenine ring, C=N(H2) for guanine and C=N7 for guanine.

Based on the data in Table S-I and Fig. S-8 and Fig. S-9, it can be concluded that the most pronounced changes are in the relative intensity of thymine ring. Additionally, guanine bands are more sensitive to small BAE–Ct-DNA. In the 1100–800 cm^{-1} region, there was a shift in the 1028 cm^{-1} band (most likely corresponding to the deoxyribose ring) to 1030 cm^{-1}. For BAE–Ct-DNA and C–O of deoxyribose, a slight shift and a 10 cm^{-1} shift in the 1105 cm^{-1} band (arising from the symmetric vibration of the O=P=O group) were observed. Thus, our data revealed the preferred binding of BAE to guanine bases and demonstrated good agreement with previous results. The structures of free Ct-DNA alone and upon interaction with BAE were quantitatively analyzed by fitting analysis, and the results are presented in Table S-I. These results are consistent with the FT-IR spectroscopy findings, which showed that BAE binding induces structural changes in Ct-DNA.[37]

Molecular docking studies

Molecular docking is a valuable tool for validating experimental data and providing deeper insight into ligand–Ct-DNA interactions. Molecular modeling was performed to predict the possible orientation of the newly formed complex between the Ct-DNA and the ligand. The interaction of Ct-DNA with ligands is shown in Figs. 2 and S-10 of the Supplementary material. It is caused by hydrophobic forces and hydrogen bonds.[38,39] The ligand can slide between DG4 and N3 with –29.4 kJ mol^{-1} into the Ct-DNA; this mode, which has the lowest

energy and the highest binding affinity, was chosen as the most favorable binding site. Therefore, it can be concluded that the results of molecular binding can further confirm the above experimental results.

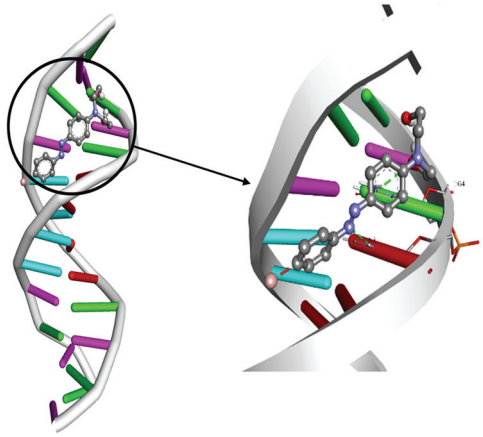

Fig. 2. Complex structure used in molecular docking.

The azo dye molecule is embedded within the groove of the Ct-DNA. The molecule is aligned along the groove without significant disruption of base stacking, indicating that it fits into the DNA structure without being inserted between base pairs. This observation is supported by the ligplot (Fig. S-10), which highlights specific hydrogen bonding and van der Waals interactions between the azo compound (Unk1) and nearby nucleotide residues (such as dg22 and dc23). A hydrogen bond at a distance of 3.06 Å further confirms the stable, non-covalent interaction typically observed in groove binders. The positions near the sugar--phosphate backbone and bases such as dc21, da6 and dg4 also align with minor groove accessibility. Collectively, these data strongly indicate that the azo dye interacts with Ct-DNA through minor groove binding, which is stabilized by hydrogen bonding and hydrophobic interactions. This type of interaction is particularly relevant in biophysical studies, as it may influence Ct-DNA conformation and gene expression without causing strand separation, making azo dyes potential candidates for gene-targeted diagnostics or therapeutics.[40]

CONCLUSION

The binding interactions between the monoazo dispersion dye (BAE) and Ct-DNA were thoroughly investigated, in this study, using molecular docking in conjunction with a variety of biophysical techniques. FT-IR spectroscopy, fluorescence and UV–Vis absorption analyses confirmed the formation of the BAE––Ct-DNA complex, and the calculated binding constant (~10^6 M^{-1}) is consistent with a groove-binding mode. Förster resonance energy transfer (FRET) analysis

showed a donor–acceptor distance of 2.99 nm between EB–Ct-DNA and BAE, indicating close proximity suitable for energy transfer. Thermodynamic parameters indicated that the binding is primarily entropy-driven ($\Delta S° > 0$) and endothermic ($\Delta H° > 0$), with the spontaneous nature of the interaction supported by negative free energy changes ($\Delta G° < 0$). Additionally, thermodynamic characteristics indicated that hydrophobic forces dominate the binding interaction, with hydrogen bonding playing a minimal role. This conclusion was corroborated by molecular docking experiments, which demonstrated a favorable binding energy and particular interactions between BAE and guanine-rich areas inside the DNA minor groove. Crucially, FT-IR spectroscopy revealed significant alterations in the thymine ring and phosphate backbone vibrational frequencies, suggesting that BAE interacts with DNA *via* the minor groove.

These results collectively offer strong proof that BAE primarily binds to Ct--DNA through minor groove binding, which is maintained by hydrogen bonding and hydrophobic interactions. This study advances our knowledge of azo dyes' DNA-binding capabilities and establishes a framework for future research into their biological activity and possible genotoxic consequences.

SUPPLEMENTARY MATERIAL

Additional data and information are available electronically at the pages of journal website: https://www.shd-pub.org.rs/index.php/JSCS/article/view/13313, or from the corresponding author on request.

Acknowledgement. This work has been supported by the University of Guilan.

ИЗВОД

ИСПИТИВАЊЕ ВЕЗИВАЊА АЗО БОЈЕ ЗА ДНК ПРИМЕНОМ СПЕКТРОСКОПСКИЈЕ И МЕТОДЕ МОЛЕКУЛСКОГ МОДЕЛОВАЊА

SHABNAM JAMPOUR-KOLOUR и HAMID DEZHAMPANAH

Department of Applied Chemistry, Faculty of Chemistry, University of Guilan, P.O.B. 1914, Rasht 0098, Iran

У овој студији је испитивана интеракција између синтетисане моноазо дисперзне боје и ДНК тимуса телета (Ct-DNA) применом UV–Vis, флуоресцентне и FT-IR спектроскопије и молекулског моделовања. На апсорпционим и флуоресцентним спектрима је уочен хипохромни ефекат и ефекат гашења, што је потврдило везивање азо боје за Ct-DNA. Након везивања за ДНК, азо боја је изазвала хипохромни ефекат и мало померање спектра ка црвеном делу, што је указало да везивање обухвата жљеб ДНК и накнадно је потврђено резултатима молекулског моделовања. Израчунате су константе везивања из интензитета максимума апсорпционих спектара за азо боју и различите концентрације Ct-DNA, на неколико температура, као и термодинамички параметри $\Delta G°$, $\Delta H°$ и $\Delta S°$. Флуоресцентни резонантни енергетски трансфер је показао да је размак између донора (Ct-DNA) и акцептора (азо боја) одговарајући за пренос енергије. Молекулско моделовање је показало да су водоничне везе и π-електрони бензеновог прстена азо боје кључни за везивање. Резултати молекулског моделовања потврђују резултате спектралне анализе, односно да се боја везује за мали жљеб Ct-DNA.

(Примљено 28. марта, ревидирано 10. априла, прихваћено 16. јула 2025)

REFERENCES

1. A. Travers , G. Muskhelishvili, *FEBS J.* **282** (2015) 2279 (https://doi.org/10.1111/febs.13307)
2. C. Nieuwland, T. A. Hamlin , C. F. Guerra , G. Barone , F. M. Bickelhaupt, *Chem. Open* **11** (2022) 2 (https://doi.org/10.1002/open.202100231)
3. S. Minchin, J. Lodge, *Essays Biochem.* **63** (2019) 433 (https://doi.org/10.1042/EBC20180038)
4. S. Gupta, S. Aggarwal, M. Munde, *ACS Omega* **8** (2023) 4554 (http://doi.org/10.1021/acsomega.2c01557)
5. K. Shridhar, G. K.Walia, A. Aggarwal, S. Gulati, A. Geetha, D. Prabhakaran, P. K. Dhillon, P. Rajaraman, *Oral Oncology* **53** (2016) 1 (http://doi.org/10.1016/j.oraloncology.2015.11.012)
6. S. Benkhaya, S. E. Mrabet, A. Harfi, *Heliyon* **6** (2020) 03271 (http://doi.org/10.1016/j.heliyon.2020.e03271)
7. Y. X. Liu, H. W. Mo, Z. Lv, F. Shen, C. L. Zhan, Y. Y. Qi, Z. Mao, X. Y. Le, *Trans. Met. Chem*. **43** (2018) 259 (http://doi.org/10.1007/s11243-018-0211-y)
8. M. Maliyappa, J. Keshavayya, N. Mallikarjuna, P. M. Krishna, N. Shivakumara, T. Sandeep, K. Sailaja, M. A. Nazrulla, *J. Mol Struct*. **1179** (2019) 630 (http://doi.org/10.1016/j.molstruc.2018.11.041)
9. A. S. Mondal, A. K. Pramanik, L. Patra, C. K. Manna, T. K. Mondal, *J. Mol. Struct.* **1146** (2017) 146 (http://doi.org/10.1016/j.molstruc.2017.05.131)
10. Y. Ali, S. Abd Hamid, U. Rashid, *Med. Chem.* **18** (2018) 1548 (http://doi.org/10.2174/1389557518666180524113111)
11. M. Y. Zhao, Y. F. Tang, G. Z. Han, *Molecules* **28** (2023) 6741 (http://doi.org/10.3390/molecules28186741)
12. N. Venugopal, G. Krishnamurthy, H. S. Bhojya Naik, J. D. Manohara, *J. Inorg. Organomet. Polym. Mat.* **30** (2020) 2608 (http://doi.org/10.1007/s10904-019-01394-8)
13. S. Qamar, Z. Akhter, S. Yousuf, H. Bano, F. Perveen, *J. Mol. Struct*. **1197** (2019) 345 (https://doi.org/10.1016/j.molstruc.2019.07.069)
14. S. Benkhaya, S. M'rabet, A. El Harfi. *Heliyon* **6** (2020) 3072. (https://doi.org/10.1016/j.heliyon.2020.e03271)
15. S. Das, S. Chatterjee, S. Pramanik, P. S. Devi, G. S. Kumar, *J. Photochem. Photobiol., B* **178** (2018) 339 (https://doi.org/10.1016/j.jphotobiol.2017.10.039)
16. M. R. Yazdanbakhsh, A. Mohammadi, *J. Mol. Liq*. **148** (2009) 35 (http://doi.org/10.1016/j.molliq.2009.06.001)
17. J. Albani, *Principles and applications of fluorescence spectroscopy*, Wiley-Blackwell, Hoboken, NJ, 2007 (http://doi.org/10.1002/9780470692059)
18. B. Kavitha, M. Sravanthi, P. Saritha Redd, *J. Mol. Struct*. **1185** (2019) 153 (https://doi.org/10.1016/j.molstruc.2019.02.093)
19. L. Hana, Y. Zhoub, X. Huangb, M. Xiaoa, L. Zhoua, J. Zhoua, A. Wangc, J. Shena, *Spectrochim. Acta, A* **123** (2014) 497 (http://dx.doi.org/10.1016/j.saa.2013.11.088)
20. X. Li, Y. Yuan, Y. Wang, F. Zhang, R. Zhao, D. Shao, S. Bi, *Process Biochem*. **108** (2021) 26 (http://doi.org/10.1016/j.procbio.2021.05.023)
21. J. Antosiewicz, D. Shugar, *Biophys. Rev*. **8** (2016) 163 (http://doi.org/10.1007/s12551-016-0197-7)
22. Y. Pin, Z. Chunqiong, *Acta Chim. Sin.* **61** (2003) 1455 (in Chinese) (https://sioc-journal.cn/Jwk_hxxb/EN/Y2003/V61/I9/1455#1)

23. Z. Shokohi-Pour, H. Chiniforoshan, M. R. Sabzalian, S. A. Esmaeili, A. A. Momtazi--Borojeni, *J. Biomol. Struct. Dyn*. **36** (2018), 532 (http://dx.doi.org/10.1080/07391102.2017.1287006)
24. K. Xia, G. Zhang, S. Li, D. Gong, *J. Fluoresc*. **27** (2017) 1815 (http://doi.org/10.1007/s10895-017-2119-x)
25. P. D. Ross, S. Subramanian, *Biochemistry* **20** (1981) 3096 (http://doi.org/10.1021/bi00514a017)
26. B. Shen, H. Yang, J. C. X. Liu, M. Zhou, *Spectrochim. Acta, A* **261** (2021) 1386 (https://doi.org/10.1016/j.saa.2021.119998)
27. S. Ansari, I. Yousuf, F. Arjmand, M. K. Siddiqi, S. Naqvi, *Int. J. Biol. Macromol*. **116** (2018) 1105 (http://doi.org/10.1016/j.ijbiomac.2018.05.052)
28. W. R. Ware, *J. Phys. Chem.* **66** (1962) 455 (https://doi.org/10.1021/j100809a020)
29. W. He, Y. Li, J. Tang, F. Luan, J. Jin, Z. Hu, *Int. J. Biol. Macromol*. **39** (2006) 165 (https://doi.org/10.1016/j.ijbiomac.2005.11.003)
30. X. Y. Cao, S. Wang, S. Q. Tian, H. Lou, Y. C. Kong, Z. J. Yang, J. L. Liu, *Spectrochim. Acta, A* **203** (2018) 301 (http://doi.org/10.1016/j.saa.2018.05.091)
31. S. S. Ansari, I. Yousuf, F. Arjmand, M. K. Siddiqi, S. Naqvi, *Int. J. Biol. Macromol*. **116** (2018) 1105 (http://doi.org/10.1016/j.ijbiomac.2018.05.052)
32. H. Li, H. Dou, Y. Zhang, Z. Li, R. Wang, J. Chang, *Spectrochim. Acta, A* **136** (2015) 416 (https://doi.org/10.1016/j.saa.2014.09.051)
33. N. Vandenberk, A. Barth, D. Borrenberghs, J. Hofkens, J. Hendrix, *J. Phys. Chem., B* **122** (2018) 4249 (http://doi.org/10.1021/acs.jpcb.8b00108)
34. X. Li, Y. Yuan, Y. Wang, F. Zhang, R. Zhao, D. Shao, S. Bi, *Process Biochem*. **108** (2021) 26–33 (https://doi.org/10.1016/j.procbio.2021.05.023)
35. *Principles of Fluorescence Spectroscopy*, 3rd ed., J. R. Lakowicz, Ed., Springer, Boston, MA, 2006 (http://doi.org/10.1007/978-0-387-46312-4)
36. S. Bi, X. Li, Z. Ren, B. Yang, Y. Wang, F. Zhang, Y. Yuan, D. Shao, R. Zhao, *Luminescence* **37** (2022) 1275 (http://doi.org/10.1002/bio.4293)
37. E. Tymchenko, V. Glova, A. Soldatova, E. Chikhirzhina, A. Polyanichko, *J. Phys.: Conf. Ser.* **1400** (2019) 1742 (http://doi.org/10.1088/1742-6596/1400/3/033004)
38. S. Ponkarpagam, K. N. Vennila, K. P. Elango, *Spectrochim. Acta, A* **278** (2022) 121351 (http://doi.org/10.1016/j.saa.2022.121351)
39. B. Shen, H. Yang, J. Chen, X. Liu, M. Zhou, *Spectrochim. Acta, A* **261** (2021) 119998 (https://doi.org/10.1016/j.saa.2021.119998)
40. E. S. Istifli, *Colorants* **1** (2022) 236 (https://doi.org/10.3390/colorants1020015).